TASK-AWARE INFORMATION ROUTING FROM COMMON REPRESENTATION SPACE IN LIFELONG LEARNING

Anonymous authors
Paper under double-blind review

ABSTRACT

Intelligent systems deployed in the real world suffer from catastrophic forgetting when exposed to a sequence of tasks. Humans, on the other hand, acquire, consolidate, and transfer knowledge between tasks that rarely interfere with the consolidated knowledge. Accompanied by self-regulated neurogenesis, continual learning in the brain is governed by the rich set of neurophysiological processes that harbor different types of knowledge, which are then integrated by the conscious processing. Thus, inspired by the Global Workspace Theory of conscious information access in the brain, we propose TAMiL[1], a continual learning method that entails task-attention modules to capture task-specific information from the common representation space. We employ simple, undercomplete autoencoders to create a communication bottleneck between the common representation space and the global workspace, allowing only the task-relevant information to the global workspace, thus greatly reducing task interference. Experimental results show that our method outperforms state-of-the-art rehearsal-based and dynamic sparse approaches and bridges the gap between fixed capacity and parameter isolation approaches while being scalable. We also show that our method effectively mitigates catastrophic forgetting while being well-calibrated with reduced task-recency bias.

1 INTRODUCTION

Deep neural networks (DNNs) deployed in the real world are normally required to learn multiple tasks sequentially and are exposed to nonstationary data distributions. Throughout their lifespan, such systems must acquire new skills without compromising previously learned knowledge. However, continual learning (CL) over multiple tasks violates the i.i.d. (independent and identically distributed) assumption on the underlying data, leading to overfitting on the current task and catastrophic forgetting of previous tasks. The menace of catastrophic forgetting occurs due to the stability-plasticity dilemma: the extent to which the system must be stable to retain consolidated knowledge and be plastic to assimilate new information (Mermillod et al., 2013). As a consequence of catastrophic forgetting, performance on previous tasks often drops significantly; in the worst case, previously learned information is completely overwritten by the new one (Parisi et al., 2019).

Humans, however, excel at CL by incrementally acquiring, consolidating, and transferring knowledge across tasks (Bremner et al., 2012). Although there is gracious forgetting in humans, learning new information rarely causes catastrophic forgetting of consolidated knowledge (French, 1999). CL in the brain is governed by a rich set of neurophysiological processes that harbor different types of knowledge, and conscious processing integrates them coherently (Goyal & Bengio, 2020). Self-regulated neurogenesis in the brain increases the knowledge bases in which information related to a task is stored without catastrophic forgetting (Kudithipudi et al., 2022). Global workspace theory (GWT) (Baars, 1994; 2005; Baars et al., 2021) posits that one such knowledge base is a common representation space of fixed capacity from which information is selected, maintained, and shared with the rest of the brain. When addressing the current task, the attention mechanism creates a communication bottleneck between the common representation space and the global workspace and

[1]Code will be made public after acceptance.

admits only relevant information in the global workspace (Goyal & Bengio, 2020). Such a system enables efficient CL in humans with systematic generalization across tasks (Bengio, 2017).

Several approaches have been proposed in the literature that mimic one or more neurophysiological processes in the brain to address catastrophic forgetting in DNN. Experience rehearsal (Ratcliff, 1990) is one of the most prominent approaches that mimics the association of past and present experiences in the brain. However, the performance of rehearsal-based approaches is poor under low buffer regimes, as it is commensurate with the buffer size (Bhat et al., 2022). On the other hand, parameter isolation methods (Rusu et al., 2016) present an extreme case of neurogenesis in which a new sub-network is initialized for each task, thus greatly reducing task interference. Nevertheless, these approaches exhibit poor reusability of parameters and are not scalable due to the addition of a large number of parameters per task. Therefore, the right combination of the aforementioned mechanisms governed by GWT could unlock effective CL in DNNs while simultaneously encouraging reusability and mitigating catastrophic forgetting.

Therefore, we propose *Task-specific Attention Modules in Lifelong learning (TAMiL)*, a novel CL approach that encompasses both experience rehearsal and self-regulated scalable neurogenesis. Specifically, TAMiL learns using current task samples and a memory buffer that represents data from all previously seen tasks. Additionally, each task entails a task-specific attention module (TAM) to capture task-relevant information in CL, similar to self-regulated neurogenesis in the brain. Reminiscent of the conscious information access proposed in GWT, each TAM acts as a bottleneck when transmitting information from the common representation space to the global workspace, thus reducing task interference. Unlike self-attention in Vision Transformers, we propose using a simple, undercomplete autoencoder as a TAM, thereby rendering the TAMiL scalable even under longer task sequences. Our contributions are as follows:

- We propose TAMiL, a novel CL approach that entails both experience rehearsal and self-regulated scalable neurogenesis to further mitigate catastrophic forgetting in CL.
- Inspired by GWT of conscious information access in the brain, we propose TAMs to capture task-specific information from the common representation space, thus greatly reducing task interference in Class- and Task-Incremental Learning scenarios.
- We also show a significant effect of task attention on other rehearsal-based approaches (e.g. ER, FDR, DER++). The generalizability of the effectiveness of TAMs across algorithms reinforces the applicability of GWT in computational models in CL.
- We also show that TAMiL is scalable and well-calibrated with reduced task-recency bias.

2 Related works

Rehearsal-based Approaches: Continual learning over a sequence of tasks has been a long-standing challenge, since learning a new task causes large weight changes in the DNNs, resulting in overfitting on the current task and catastrophic forgetting of older tasks (Parisi et al., 2019). Similar to experience rehearsal in the brain, early works attempted to address catastrophic forgetting through Experience-Replay (ER; Ratcliff (1990); Robins (1995)) by explicitly storing and replaying previous task samples alongside current task samples. Function Distance Regularization (FDR; Benjamin et al. (2018)), Dark Experience Replay (DER++; Buzzega et al. (2020)) and CLS-ER (Arani et al., 2022) leverage soft targets in addition to ground truth labels to enforce consistency regularization across previous and current model predictions. In addition to rehearsal, DRI (Wang et al., 2022) utilizes a generative model to augment rehearsal under low buffer regimes. On the other hand, Co^{2}L (Cha et al., 2021) and ER-ACE (Caccia et al., 2021a) modify the learning objective to prevent representation drift when encountered with new classes. Given sufficient memory, replay-based approaches mimic the association of past and present experiences in humans and are fairly successful in challenging CL scenarios. However, in scenarios where buffer size is limited, they suffer from overfitting (Bhat et al., 2022), exacerbated representation drift (Caccia et al., 2021b) and prior information loss (Zhang et al., 2020) resulting in aggravated forgetting of previous tasks.

Evolving Architectures: In addition to experience rehearsal, CL in the brain is mediated by self-regulated neurogenesis that scale up the number of new memories that can be encoded and stored without catastrophic forgetting (Kudithipudi et al., 2022). Similarly in DNNs, Progressive Neural Networks (PNNs; Rusu et al. (2016)) instantiate a new sub-network for each task with lateral

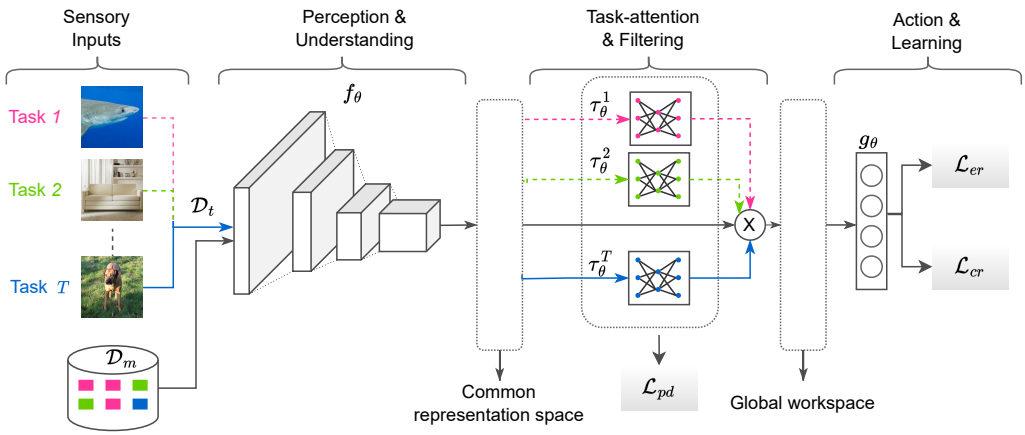

Figure 1: TAMiL encompasses both experience rehearsal and self-regulated scalable neurogenesis. For each task, the current task data $\mathcal{D}_t$ is first mapped to common representation space using f_θ. The corresponding TAM then captures the task specific information contained in $\mathcal{D}_t$ and applies transformation coefficients to select features important for the current task thereby preventing task interference. We use a matching criterion as an ignition event to trigger a particular TAM for both buffered and test samples.

connections to previously learned frozen models. Several works have been proposed to address the issue of scalability in PNNs: CCLL (Singh et al., 2020) employed a fixed capacity model and re-used the features captured on the first task by performing spatial and channel-wise calibration for all later tasks. DEN (Yoon et al., 2018) proposed a dynamically expandable network using selective re-training, network expansion with group sparsity regularization and neuron duplication. Similarly, CPG (Hung et al., 2019a) proposed an iterative approach with pruning of previous task weights followed by gradual network expansion while re-using critical weights from the previous tasks. MNTDP (Veniat et al., 2020) employed a modular learning approach to to transfer knowledge between related tasks while scaling sub-linearly with the number of tasks. Although these approaches grow drastically slower than PNNs, they require task identity at inference time. On the other hand, Mendez & Eaton (2020) explicitly captured compositional structures in lifelong learning thereby enabling their re-usability across tasks. However, this requires joint training of subset of tasks to learn initial generalizable compositional structures. Requiring task-identity at inference and joint training of subset of tasks at initialization are an impediment for deploying these CL systems in the real world.

By contrast, several other methods (e.g. NISPA (Gurbuz & Dovrolis, 2022), CLNP (Golkar et al., 2019), PackNet (Mallya & Lazebnik, 2018), PAE (Hung et al., 2019b)) proposed dynamic sparse networks based on neuronal model sparsification with fixed model capacity. Similar to the brain, these models simultaneously learn both connection strengths and a sparse architecture for each task, thereby isolating the task-specific parameters. However, these methods suffer from capacity saturation in longer task sequences, thus rendering them inapplicable to real world scenarios.

We propose TAMiL, a CL method that, while drawing inspiration from GWT, successfully combines rehearsal and parameter isolation with little memory overhead (Table 4), superior performance (Table 1) without capacity saturation, and without requiring task-identity at inference time. To the best of our knowledge, our work is the first to study GWT-inspired CL approach to effectively mitigate catastrophic forgetting.

3 Proposed Method

3.1 Preliminary

We consider a CL setting in which multiple sequential tasks $t \in \{1, 2, .., T\}$ are learned by the model Φ_θ one at a time. Each task is specified by a task-specific distribution $\mathcal{D}_t$ with $\{(x_i, y_i)\}_{i=1}^{N}$ pairs.

In this training paradigm, any two task-specific distributions are disjoint. The model Φ_θ consists of a backbone network f_θ and a classifier g_θ that represents classes belonging to all tasks. The learning objective in such an CL setting is to restrict the empirical risk of all tasks seen so far:

$$\mathcal{L}_t = \sum_{t=1}^{T_c} \mathop{\mathbb{E}}_{(x_i,y_i)\sim\mathcal{D}_t} \left[\mathcal{L}_{ce}(\sigma(\Phi_\theta(x_i)), y_i)\right], \tag{1}$$

where $\mathcal{L}_{ce}$ is a cross-entropy loss, t is the current task, and σ is the softmax function. Critically, sequential learning causes significant weight changes in Φ_θ in subsequent tasks, resulting in catastrophic forgetting of previous tasks and overfitting on the current task if Φ_θ is trained on each task only once in its lifetime without revisiting them. To mitigate catastrophic forgetting in CL, we employ experience rehearsal along with consistency regularization through episodic replay. Central to our method are the Task-specific Attention Modules (TAMs) that attend to important features of the input. We define two representation spaces namely common representation space and global workspace that are spanned by mapping functions $\mathcal{M}_f : \mathbb{R}^{B,H,W,C} \rightarrow \mathbb{R}^D$ and $\mathcal{M}_{_{TAM}} : \mathbb{R}^D \rightarrow \mathbb{R}^D$ where D denotes the dimension of output Euclidean space. $\mathcal{M}_f$ is a set of possible functions that the encoder f_θ can learn whereas $\mathcal{M}_{_{TAM}}$ denotes a set of functions represented by TAMs. We use simple undercomplete autoencoders as task-specific attention modules that can act as feature selectors. We describe each of these components shown in Figure 1 in the following sections.

3.2 Episodic Replay

To preserve knowledge of previous tasks, we seek to approximate previous data distributions $\mathcal{D}_{t\in\{t:1\leq i<T_c\}}$ through a memory buffer $\mathcal{D}_m$ with reservoir sampling (Vitter, 1985). Each sample in $\mathcal{D}_t$ has the same probability of being represented in the buffer and replacements are performed randomly. At each iteration, we randomly sample from $\mathcal{D}_m$ and replay them along with $\mathcal{D}_t$. Therefore, the objective function in Eq. 1 can be conveniently modified as follows:

$$\mathcal{L}_{er} = \mathcal{L}_{T_c} + \alpha \mathop{\mathbb{E}}_{(x_j,y_j)\sim\mathcal{D}_m} \left[\mathcal{L}_{ce}(\sigma(\Phi_\theta(x_j)), y_j)\right], \tag{2}$$

where α is a balancing parameter. Experience rehearsal improves stability that is commensurate with the ability of $\mathcal{D}_m$ to approximate past distributions. In scenarios where buffer size is limited, the CL model learns sample-specific features rather than capturing class- or task-wise representative features, resulting in poor performance under low buffer regimes. As soft targets carry more information per training sample than hard targets, we therefore employ consistency regularization Bhat et al. (2022) (Action & Learning in Figure 1) to better preserve the information from previous tasks. We straightforwardly define consistency regularization using mean squared error as follows:

$$\mathcal{L}_{cr} \triangleq \mathop{\mathbb{E}}_{(x_j,y_j,z_j)\sim D_m} \|z_j - \Phi_\theta(x_j)\|_2^2 \tag{3}$$

where z_j represents the pre-softmax responses of an Exponential Moving Average (EMA) of the CL model. Alternatively, z_j from previous iterations can also be stored in the buffer.

3.3 Task-specific Attention Modules In Lifelong learning (TAMiL)[2]

Reminiscent of the conscious information access proposed in GWT, we propose task-specific attention modules (TAMs) (Task attention & Filtering in Figure 1) to capture task-relevant information in CL. Following Stephenson et al. (2020), we believe that the common representation space spanned by $\mathcal{M}_f$ captures generic information relevant for all tasks while TAMs capture task-specific information. The choice of these attention modules should be such that there is enough flexibility for them to capture task-relevant information, and they are diverse enough to differentiate between tasks during inference while still rendering the CL model scalable in longer task sequences. To this end, we propose using simple undercomplete autoencoders as TAMs. Each of these TAMs consists of two parts $\tau_\theta^i = \{\tau_\theta^{ie}, \tau_\theta^{is}\}$, where τ_θ^{ie} acts as a feature extractor and τ_θ^{is} as a feature selector. The feature extractor learns a low-dimensional subspace using a linear layer followed by ReLU activation. On the other hand, the feature selector learns task-specific attention using another linear layer followed by sigmoid activation. The bottleneck in the proposed TAMs achieves twin objectives: (i)

[2]TAMs have similar structure as autoencoders but do not reconstruct the input

Algorithm 1 Proposed Method

input: Data streams $\mathcal{D}_t$, Model $\Phi_\theta = \{f_\theta, \tau_\theta, g_\theta\}$, Balancing factors α, β and λ
Memory buffer $\mathcal{D}_m \leftarrow \{\}$, TAMs $\tau_\theta \leftarrow \{\}$

for all tasks $t \in \{1, 2, .., T\}$ **do**
  $\tau_\theta = \tau_\theta \cup \{\tau_\theta^t\}$
  for minibatch $\{x_i, y_i\}_{i=1}^B \in \mathcal{D}_t$ **do**
    $\hat{y}_i = g_\theta(\tau_\theta^t(f_\theta(x_i)) \otimes f_\theta(x_i))$
    Compute $\mathcal{L}_{er} = \frac{1}{B} \sum_B \mathcal{L}_{ce}(\hat{y}_i, y_i)$ ▷ (Equation 2)
    Compute $\mathcal{L}_{pd}$ ▷ (Equation 4)
    if $\mathcal{D}_m \neq \emptyset$ **then**
      for minibatch $\{x_j, y_j, z_j\}_{j=1}^B \in \mathcal{D}_m$ **do**
        $r_m = f_\theta(x_j)$
        $k = \underset{k \in 1,..,t}{\text{argmin}} \; \|\tau_\theta^k(r_m) - r_m\|_2^2$ ▷ (Equation 5)
        $\hat{y}_j = g_\theta(\tau_\theta^k(r_m) \otimes r_m)$
        Compute $\mathcal{L}_{er} \; += \frac{\alpha}{B} \sum_B \mathcal{L}_{ce}(\hat{y}_j, y_j)$ ▷ (Equation. 2)
        Compute $\mathcal{L}_{cr}$ ▷ (Equation 3)
    Compute $\mathcal{L} \triangleq \mathcal{L}_{er} + \beta \, \mathcal{L}_{cr} - \lambda \, \mathcal{L}_{pd}$ ▷ (Equation. 6)
    Compute the gradients $\frac{\delta \mathcal{L}}{\delta \theta}$ and update the model Φ_θ
    Update the memory buffer $\mathcal{D}_m$ ▷ (Algorithm 2)
return model Φ_θ

it inhibits TAMs from reconstructing their own input, (ii) while reducing the number of parameters required to learn task-relevant information. Similar to neurogenesis in the brain, TAMs encode and store task-specific attention while still being scalable to a large number of tasks.

To effectively leverage the functional space of TAMs, we seek to maximize pairwise discrepancy loss between output representations of the TAMs trained so far:

$$\mathcal{L}_{pd} \triangleq \sum_{t=1}^{T_c - 1} \mathop{\mathbb{E}}_{x \sim D_t} \|\sigma(\tau_\theta^{T_c}(r)) - stopgrad(\sigma(\tau_\theta^t(r)))\|_{p=1} \tag{4}$$

where $r = f_\theta(x)$ is the representation in the common representation space. As a stricter pairwise discrepancy could result in capacity saturation and reduce flexibility to learn new tasks, we employ the softmax function $\sigma(.)$ while enforcing diversity between TAMs. We also update the gradients of only the current TAM τ_θ^t to avoid overwriting the previous task attention using *stopgrad(.)*. Without Eq. 4, multiple TAMs can be very similar, reducing their effectiveness as task-specific attention.

3.4 PUTTING IT ALL TOGETHER

3.4 Putting it all together

TAMiL consists of a CL model $\Phi_\theta = \{f_\theta, \tau_\theta, g_\theta\}$ where f_θ represents a feature extractor (e.g. ResNet-18), $\tau_\theta = \{\tau_\theta^k \mid k \leq t\}$ is a set of TAMs up to the current task t, and the classifier g_θ represents classes belonging to all tasks. Analogous to the common representation space proposed in GWT, we employ f_θ as a common representation space to capture sensory information $\mathcal{D}_t$ from all tasks sequentially. For each task, a new TAM is initialized that acts as a feature selector by attending to features important for the given task. The intuition behind placing the TAMs higher up in the layer hierarchy is as follows: The early layers of DNNs capture generic information, while the later layers memorize due to diminishing manifold dimension and radius (Stephenson et al., 2020; Baldock et al., 2021). Therefore, redundancy in the later layers is desirable to reduce catastrophic forgetting while maximizing reusability.

The goal of TAMs is to act as a task-specific bottleneck through which only task-relevant information is sent through the global workspace spanned by $\mathcal{M}_{TAM}$. Specifically, during CL training, the

corresponding TAM learns to weigh the incoming the features based on the task identifier using current task data $\mathcal{D}_t$. The output of the corresponding TAM termed as transformation coefficients are then applied to the features of the common representation space using element-wise multiplication. Furthermore, we enforce the pairwise discrepancy loss in Eq. 4 to ensure the diversity among TAMs. On the downside, since each TAM is associated with a specific task, inferring a wrong TAM for the test samples can result in sub-par performance on the test set.

In the brain, information is not always processed consciously unless there is sufficient activation in the prefrontal region, resulting in an ignition event (Juliani et al., 2022). Analogously, we emulate the ignition event with a matching criterion using buffered samples from $\mathcal{D}_m$. During training, for each buffered sample, we infer the identity of the task by computing the mean squared error between the feature r_m of the common representation space and the output of each of the TAMs seen so far. We select the TAM with the lowest matching criterion as follows:

$$\underset{k \in 1,..,t}{\operatorname{argmin}} \; \|\tau_\theta^k(r_m) - r_m\|_2^2 \tag{5}$$

where $r_m = f_\theta(x_j)$, $x_j \in \mathcal{D}_m$. Once the right TAM is selected, we apply cross-entropy loss (Eq. 2) and consistency regularization (Eq. 3) on the buffered samples. As the CL model is now trained to select the appropriate TAM, we also use the same criterion during the inference stage. We selected the matching criterion as an ignition event due to its simplicity and lack of additional trainable parameters. However, complex alternatives such as learning a policy using reinforcement learning, a gating mechanism using Gumbel-softmax, and prototype matching can also be explored.

In addition to $\mathcal{L}_{pd}$ (Eq. 4), we do not use any other objective on the TAMs to constrain their learning. The final learning objective for the entire CL model is as follows:

$$\mathcal{L} \triangleq \mathcal{L}_{er} + \beta \, \mathcal{L}_{cr} - \lambda \, \mathcal{L}_{pd} \tag{6}$$

Our proposed approach is illustrated in Figure 1 and is detailed in Algorithm 1.

4 Experimental setup

We build on top of the Mammoth (Buzzega et al., 2020) CL repository in PyTorch. We consider two CL scenarios, namely, Class-Incremental Learning (Class-IL) and Task-Incremental Learning (Task-IL). In a Class-IL setting, the CL model encounters mutually exclusive sets of classes in each task and must learn to distinguish all classes encountered thus far by inferring the task identity. In contrast, the task identity is always provided during both training and inference in the Task-IL scenario. More information on the details of the implementation can be found in Appendix E. In the empirical results, we compare with several state-of-the-art rehearsal-based methods and report average accuracy after learning all the tasks. As our method employs consistency regularization, we also compare with the popular regularization-based method LwF (Li & Hoiem, 2017). In addition, we provide a lower bound SGD, without any help to mitigate catastrophic forgetting, and an upper bound Joint, where training is done using entire dataset. In the *Oracle* version, for any test sample $x \in \mathcal{D}_t$, we use task identity at inference time to select the right TAM.

5 Results

Table 1 presents the evaluation of different CL models on multiple sequential datasets. We can make several observations: (i) Across all datasets, TAMiL outperforms all the rehearsal-based baselines considered in this work. As is the case in GWT, TAMs capture task-specific features and reduce interference, thereby enabling efficient CL with systematic generalization across tasks. For example, in the case of Seq-TinyImageNet with buffer size 500, the absolute improvement over the closest baseline is $\sim 10\%$ in both CL scenarios. (ii) The performance improvement in Class-IL is even more pronounced when we know the identity of the task (Oracle version). Notwithstanding their size, this is a testament to the ability of TAMs to admit only relevant information from the common representation space to the global workspace when warranted by a task-specific input. (iii) Given the bottleneck nature of TAMs, the additional parameters introduced in each task are negligible in size compared to the parameter growth in PNNs. However, TAMiL bridges the performance gap between rehearsal-based and parameter-isolation methods without actually incurring a large

computational overhead. Given sufficient buffer size, our method outperforms PNNs.(e.g. in case of Seq-CIFAR100 with buffer size 500, our method outperforms the PNNs.)

Table 1: Comparison of CL models across various CL scenarios. We provide the average Top-1 (%) accuracy of all tasks after CL training. Forgetting analysis can be found in Appendix D.2.

Buffer size	Methods	Seq-CIFAR10		Seq-CIFAR100		Seq-TinyImageNet	
		Class-IL	Task-IL	Class-IL	Task-IL	Class-IL	Task-IL
-	SGD	19.62±0.05	61.02±3.33	17.49±0.28	40.46±0.99	07.92±0.26	18.31±0.68
	Joint	92.20±0.15	98.31±0.12	70.56±0.28	86.19±0.43	59.99±0.19	82.04±0.10
-	LwF	19.61±0.05	63.29±2.35	18.47±0.14	26.45±0.22	8.46±0.22	15.85±0.58
	PNNs	-	95.13±0.72	-	74.01±1.11	-	67.84±0.29
200	ER	44.79±1.86	91.19±0.94	21.40±0.22	61.36±0.35	8.57±0.04	38.17±2.00
	FDR	30.91±2.74	91.01±0.68	22.02±0.08	61.72±1.02	8.70±0.19	40.36±0.68
	DER++	64.88±1.17	91.92±0.60	29.60±1.14	62.49±1.02	10.96±1.17	40.87±1.16
	Co^{2}L	65.57±1.37	93.43±0.78	31.90±0.38	55.02±0.36	13.88±0.40	42.37±0.74
	ER-ACE	62.08±1.44	92.20±0.57	35.17±1.17	63.09±1.23	11.25 ± 0.54	44.17 ±1.02
	CLS-ER[1]	61.88±2.43	93.59±0.87	-	-	17.68±1.65	52.60±1.56
	DRI	65.16±1.13	92.87±0.71	-	-	17.58±1.24	44.28±1.37
	TAMiL	**68.84**±1.18	**94.28**±0.31	**41.43**±0.75	**71.39**±0.17	**20.46**±0.40	**55.44**±0.52
	TAMiL (Oracle)	**91.08**±0.91	91.08 ±0.91	**71.21**±0.27	**71.68**±0.15	**54.41**±0.49	**55.78**±0.75
500	ER	57.74±0.27	93.61±0.27	28.02±0.31	68.23±0.17	9.99±0.29	48.64±0.46
	FDR	28.71±3.23	93.29±0.59	29.19±0.33	69.76±0.51	10.54±0.21	49.88±0.71
	DER++	72.70±1.36	93.88±0.50	41.40±0.96	70.61±0.08	19.38±1.41	51.91±0.68
	Co^{2}L	74.26±0.77	**95.90**±0.26	39.21±0.39	62.98±0.58	20.12±0.42	53.04±0.69
	ER-ACE	68.45±1.78	93.47±1.00	40.67±0.06	66.45±0.71	17.73 ± 0.56	49.99 ±1.51
	CLS-ER[1]	70.40±1.21	94.35±0.38	-	-	24.97±0.80	61.57±0.63
	DRI	72.78±1.44	93.85±0.46	-	-	22.63±0.81	52.89±0.60
	TAMiL	**74.45**±0.27	94.61±0.19	**50.11**±0.34	**76.38**±0.30	**28.48**±1.50	**64.42**±0.27
	TAMiL (Oracle)	**93.93**±0.38	93.93±0.38	**76.75**±0.12	**76.88**±0.11	**64.06**±2.38	**64.55**±2.14

[1] Single EMA model.

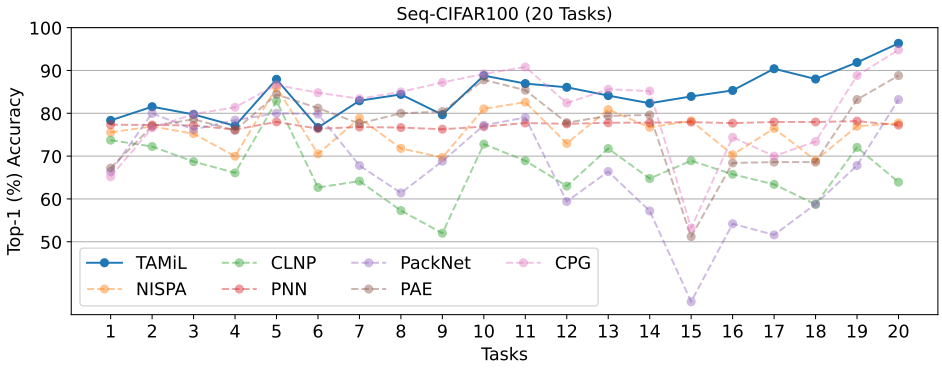

Figure 2: Comparison of final task accuracy of dynamic sparse approaches after training on Seq-CIFAR100 in 20 tasks. For TAMiL, we use a buffer size of 500. TAMiL outperforms dynamic sparse approaches with fixed model capacity by a large margin.

Comparison with dynamic sparse networks: Similar to PNNs, dynamic sparse networks reduce task interference by learning a non-overlapping task-specific sparse architecture within a fixed capacity model. We consider these two approaches to be two extremes of parameter isolation in CL, as the former suffers from scalability issues, while the latter from capacity saturation. Figure 2 presents a comparison of the final task accuracies of TAMiL with parameter isolation methods on Seq-CIFAR100 (20 tasks) under the Task-IL scenario. Although TAMiL uses a slightly bigger model (Appendix E.3), it does not suffer from capacity saturation or scalability problems and retains strong performance when exposed to a large number of tasks. As earlier layers capture task-agnostic information, parameter isolation in the later layers largely benefits TAMiL.

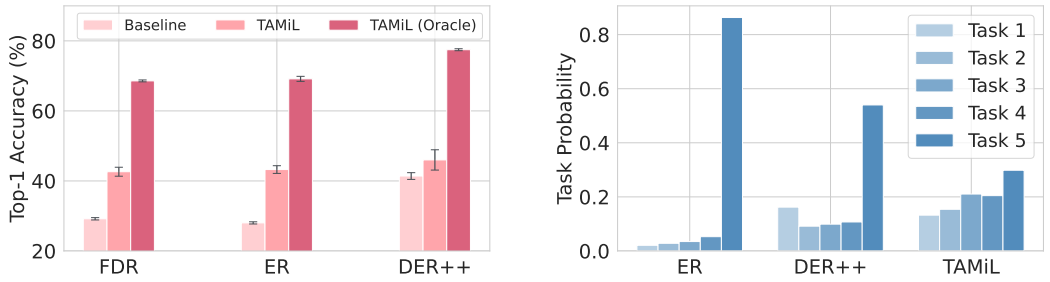

Figure 3: Left: Comparison of top-1 accuracy (%) of CL models with and without TAMs. Right: Average task probabilities of different CL models after Cl training. Both of the above experiments were done on Seq-CIFAR100 with buffer size 500.

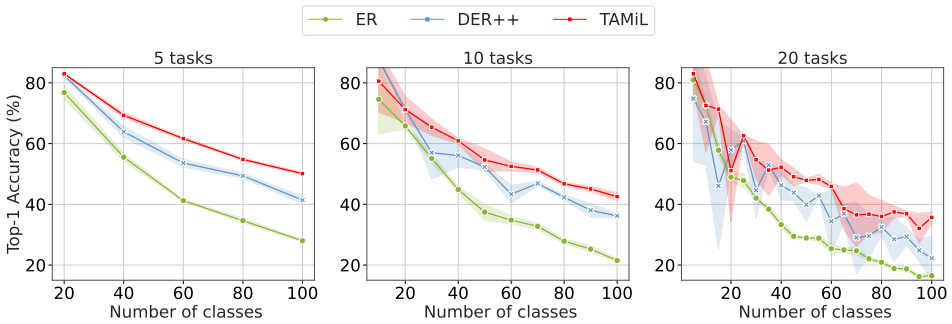

Figure 4: Comparison of Top-1 accuracy (%) of CL models in Seq-CIFAR100 with different number of tasks. TAMiL consistently outperforms the baselines under longer task sequences.

Effect of task-attention on prior art: Analogous to our method, we attempt to augment several existing rehearsal-based methods by equipping them with the TAMs. Figure 3(left) provides a comparison of CL methods with and without TAM when trained on Seq-CIFAR100 (5 tasks) with buffer size 500 in Class-IL scenario. Quite evidently, TAMs drastically improve the performance of all CL methods, more so when the true TAM is used for inference (Oracle). Independent of the underlying learning mechanism, these dedicated modules admit only the task-relevant information from the common representation space to the global workspace when warranted by a task-specific input, thereby drastically reducing interference. The generalizability of the effectiveness of TAMs across algorithms reinforces our earlier hypothesis that emulating GWT in computational models can greatly benefit CL with systematic generalization across tasks.

Task-recency bias: CL models trained in an incremental learning scenario tend to be biased toward the most recent tasks, termed task-recency bias (Hou et al., 2019). Following the analysis of recency bias in Buzzega et al. (2020); Arani et al. (2022), we present the task probabilities in Figure 3 (right). We first compute the prediction probabilities of all samples and average them. For each task, task probability stands for sum of average prediction probabilities of associated classes. The predictions of ER are biased mostly towards recent tasks, with the most recent task being almost 8X as much as the first task. On the contrary, the predictions in TAMiL are more evenly distributed than the baselines, greatly mitigating the task recency bias.

Performance under longer-task sequences: Computational systems deployed in the real world are often exposed to a large number of sequential tasks. For rehearsal-based methods with a fixed memory budget, the number of samples in the buffer representing each previous task is drastically reduced in longer sequences of tasks, resulting in poor performance, called long-term catastrophic forgetting (Peng et al., 2021). Therefore, it is quintessential for the CL model to perform well under low buffer regimes and longer task sequences. Figure 4 provides an overview of the performance of CL models with 5, 10, and 20 task sequences on Seq-CIFAR100 with a fixed buffer size of 500. As the number of tasks increases, the number of samples per class decreases, resulting in increased

Table 2: Ablations of the different key components of our proposed method. The Top-1 accuracy (%) is reported on Seq-CIFAR100 for the 500 buffer size learned with 5 tasks.

EMA Model	Pairwise loss	TAMs	Class-IL	Task-IL
✓	✓	✓	**50.11**$\pm$0.34	**76.47**$\pm$0.51
✗	✓	✓	47.51$\pm$0.96	73.79 $\pm$0.51
✗	✗	✓	45.10$\pm$3.46	73.34 $\pm$0.67
✗	✗	✗	41.40$\pm$0.96	70.61$\pm$0.08

forgetting. Our method equipped with TAMs preserves the previous task information better and exhibits superior performance over baselines even under extreme low-buffer regimes.

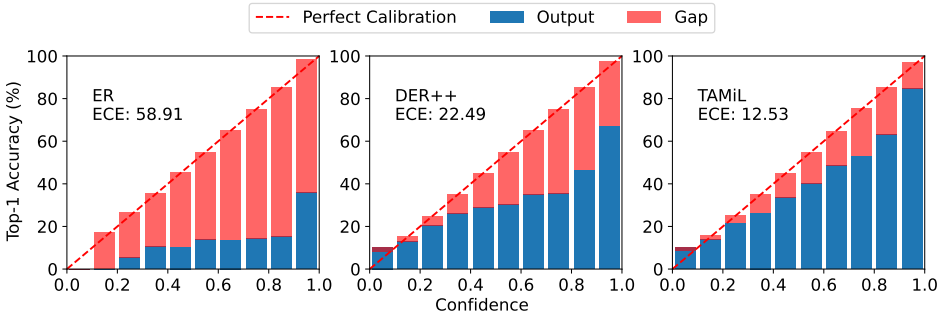

Figure 5: Reliability diagram along with ECE for different CL models trained on Seq-CIFAR100 (buffer size 500) with 5 tasks. Our approach is well-calibrated and closer to the perfect calibration when compared to the baselines.

Model calibration: It is pertinent that computational systems deployed in safety-critical environments are reliable and have an adequate sense of uncertainty about their predictions. A well-calibrated model improves reliability by reducing the expectation difference between confidence and accuracy (Guo et al., 2017). Figure 5 shows the Expected Calibration Error (ECE) along with a reliability diagram on Seq-CIFAR100 using a calibration framework (Kuppers et al., 2020). As can be seen, ER is highly miscalibrated and more overconfident than other CL models. On the other hand, TAMiL has the lowest ECE by ensuring that the predicted softmax scores are better indicators of the actual probability of a correct prediction. In addition to drastically reducing catastrophic forgetting in CL, TAMs in our approach help mitigate miscalibration, thereby improving reliability.

Ablation study: We attempt to disentangle the contribution of key components in our approach. Table 2 provides an ablation study of our method trained on Seq-CIFAR100 with buffer size 500 for 5 tasks (More ablation on TAMs can be found in Appendix A.2). When the EMA model is absent, we store past predictions in the buffer for consistency regularization. As can be seen, each component contributes significantly to the overall performance of TAMiL

6 Conclusion

We proposed TAMiL, a novel CL approach that encompasses both experience rehearsal and self-regulated scalable neurogenesis to further mitigate catastrophic forgetting in CL. Inspired by the Global Workspace theory (GWT) of conscious information access in the brain, Task-specific Attention Modules (TAMs) in our approach capture task-specific information from the common representation space, thus greatly reducing task interference. The generalizability of the effectiveness of TAMs across CL algorithms reinforces the applicability of GWT in computational models in CL. Given the bottleneck nature of TAMs, the additional parameters introduced in each task are negligible in size compared to parameter growth in PNNs. TAMiL neither suffers from capacity saturation nor scalability issues and retains strong performance even when exposed to a large number of tasks. Although TAMiL performs extremely well, more sophisticated matching criteria can be developed to shore up performance close to the oracle version in the future.

REFERENCES

Elahe Arani, Fahad Sarfraz, and Bahram Zonooz. Learning fast, learning slow: A general continual learning method based on complementary learning system. *arXiv preprint arXiv:2201.12604*, 2022.

Bernard J Baars. A global workspace theory of conscious experience. *Consciousness in philosophy and cognitive neuroscience*, pp. 149–171, 1994.

Bernard J Baars. Global workspace theory of consciousness: toward a cognitive neuroscience of human experience. *Progress in brain research*, 150:45–53, 2005.

Bernard J Baars, Natalie Geld, and Robert Kozma. Global workspace theory (gwt) and prefrontal cortex: Recent developments. *Frontiers in Psychology*, pp. 5163, 2021.

Robert Baldock, Hartmut Maennel, and Behnam Neyshabur. Deep learning through the lens of example difficulty. *Advances in Neural Information Processing Systems*, 34:10876–10889, 2021.

Yoshua Bengio. The consciousness prior. *arXiv preprint arXiv:1709.08568*, 2017.

Ari Benjamin, David Rolnick, and Konrad Kording. Measuring and regularizing networks in function space. In *International Conference on Learning Representations*, 2018.

Prashant Bhat, Bahram Zonooz, and Elahe Arani. Consistency is the key to further mitigating catastrophic forgetting in continual learning. *arXiv preprint arXiv:2207.04998*, 2022.

Andrew J Bremner, David J Lewkowicz, and Charles Spence. *Multisensory development*. Oxford University Press, 2012.

Pietro Buzzega, Matteo Boschini, Angelo Porrello, Davide Abati, and Simone Calderara. Dark experience for general continual learning: a strong, simple baseline. *Advances in neural information processing systems*, 33:15920–15930, 2020.

Lucas Caccia, Rahaf Aljundi, Nader Asadi, Tinne Tuytelaars, Joelle Pineau, and Eugene Belilovsky. New insights on reducing abrupt representation change in online continual learning. In *International Conference on Learning Representations*, 2021a.

Lucas Caccia, Rahaf Aljundi, Nader Asadi, Tinne Tuytelaars, Joelle Pineau, and Eugene Belilovsky. Reducing representation drift in online continual learning. *arXiv preprint arXiv:2104.05025*, 2021b.

Hyuntak Cha, Jaeho Lee, and Jinwoo Shin. Co2l: Contrastive continual learning. In *Proceedings of the IEEE/CVF International Conference on Computer Vision*, pp. 9516–9525, 2021.

Stanislas Dehaene, Michel Kerszberg, and Jean-Pierre Changeux. A neuronal model of a global workspace in effortful cognitive tasks. *Proceedings of the national Academy of Sciences*, 95(24): 14529–14534, 1998.

Stanislas Dehaene, Claire Sergent, and Jean-Pierre Changeux. A neuronal network model linking subjective reports and objective physiological data during conscious perception. *Proceedings of the National Academy of Sciences*, 100(14):8520–8525, 2003.

Robert M French. Catastrophic forgetting in connectionist networks. *Trends in cognitive sciences*, 3(4):128–135, 1999.

Siavash Golkar, Michael Kagan, and Kyunghyun Cho. Continual learning via neural pruning. *arXiv preprint arXiv:1903.04476*, 2019.

Anirudh Goyal and Yoshua Bengio. Inductive biases for deep learning of higher-level cognition. *arXiv preprint arXiv:2011.15091*, 2020.

Chuan Guo, Geoff Pleiss, Yu Sun, and Kilian Q Weinberger. On calibration of modern neural networks. In *International conference on machine learning*, pp. 1321–1330. PMLR, 2017.

Mustafa B Gurbuz and Constantine Dovrolis. Nispa: Neuro-inspired stability-plasticity adaptation for continual learning in sparse networks. In *International Conference on Machine Learning*, pp. 8157–8174. PMLR, 2022.

Kaiming He, Xiangyu Zhang, Shaoqing Ren, and Jian Sun. Deep residual learning for image recognition. In *Proceedings of the IEEE conference on computer vision and pattern recognition*, pp. 770–778, 2016.

Geoffrey E Hinton and Ruslan R Salakhutdinov. Reducing the dimensionality of data with neural networks. *science*, 313(5786):504–507, 2006.

Saihui Hou, Xinyu Pan, Chen Change Loy, Zilei Wang, and Dahua Lin. Learning a unified classifier incrementally via rebalancing. In *Proceedings of the IEEE/CVF Conference on Computer Vision and Pattern Recognition*, pp. 831–839, 2019.

Ching-Yi Hung, Cheng-Hao Tu, Cheng-En Wu, Chien-Hung Chen, Yi-Ming Chan, and Chu-Song Chen. Compacting, picking and growing for unforgetting continual learning. *Advances in Neural Information Processing Systems*, 32, 2019a.

Steven CY Hung, Jia-Hong Lee, Timmy ST Wan, Chein-Hung Chen, Yi-Ming Chan, and Chu-Song Chen. Increasingly packing multiple facial-informatics modules in a unified deep-learning model via lifelong learning. In *Proceedings of the 2019 on International Conference on Multimedia Retrieval*, pp. 339–343, 2019b.

Arthur Juliani, Kai Arulkumaran, Shuntaro Sasai, and Ryota Kanai. On the link between conscious function and general intelligence in humans and machines. *arXiv preprint arXiv:2204.05133*, 2022.

Giri P Krishnan, Timothy Tadros, Ramyaa Ramyaa, and Maxim Bazhenov. Biologically inspired sleep algorithm for artificial neural networks. *arXiv preprint arXiv:1908.02240*, 2019.

Alex Krizhevsky, Geoffrey Hinton, et al. Learning multiple layers of features from tiny images. 2009.

Dhireesha Kudithipudi, Mario Aguilar-Simon, Jonathan Babb, Maxim Bazhenov, Douglas Blackiston, Josh Bongard, Andrew P Brna, Suraj Chakravarthi Raja, Nick Cheney, Jeff Clune, et al. Biological underpinnings for lifelong learning machines. *Nature Machine Intelligence*, 4(3):196–210, 2022.

Fabian Kuppers, Jan Kronenberger, Amirhossein Shantia, and Anselm Haselhoff. Multivariate confidence calibration for object detection. In *Proceedings of the IEEE/CVF Conference on Computer Vision and Pattern Recognition Workshops*, pp. 326–327, 2020.

Ya Le and Xuan Yang. Tiny imagenet visual recognition challenge. *CS 231N*, 7(7):3, 2015.

Zhizhong Li and Derek Hoiem. Learning without forgetting. *IEEE transactions on pattern analysis and machine intelligence*, 40(12):2935–2947, 2017.

Chunjie Luo, Jianfeng Zhan, Xiaohe Xue, Lei Wang, Rui Ren, and Qiang Yang. Cosine normalization: Using cosine similarity instead of dot product in neural networks. In *International Conference on Artificial Neural Networks*, pp. 382–391. Springer, 2018.

Arun Mallya and Svetlana Lazebnik. Packnet: Adding multiple tasks to a single network by iterative pruning. In *Proceedings of the IEEE conference on Computer Vision and Pattern Recognition*, pp. 7765–7773, 2018.

Davide Maltoni and Vincenzo Lomonaco. Continuous learning in single-incremental-task scenarios. *Neural Networks*, 116:56–73, 2019.

Valerio Mante, David Sussillo, Krishna V Shenoy, and William T Newsome. Context-dependent computation by recurrent dynamics in prefrontal cortex. *nature*, 503(7474):78–84, 2013.

George A. Mashour, Pieter Roelfsema, Jean-Pierre Changeux, and Stanislas Dehaene. Conscious processing and the global neuronal workspace hypothesis. *Neuron*, 105(5):776–798, 2020. ISSN 0896-6273.

Jorge A Mendez and Eric Eaton. Lifelong learning of compositional structures. In *International Conference on Learning Representations*, 2020.

Martial Mermillod, Aurélia Bugaiska, and Patrick Bonin. The stability-plasticity dilemma: Investigating the continuum from catastrophic forgetting to age-limited learning effects, 2013.

German I Parisi, Ronald Kemker, Jose L Part, Christopher Kanan, and Stefan Wermter. Continual lifelong learning with neural networks: A review. *Neural Networks*, 113:54–71, 2019.

Jian Peng, Bo Tang, Hao Jiang, Zhuo Li, Yinjie Lei, Tao Lin, and Haifeng Li. Overcoming long-term catastrophic forgetting through adversarial neural pruning and synaptic consolidation. *IEEE Transactions on Neural Networks and Learning Systems*, 2021.

Roger Ratcliff. Connectionist models of recognition memory: constraints imposed by learning and forgetting functions. *Psychological review*, 97(2):285, 1990.

Anthony Robins. Catastrophic forgetting, rehearsal and pseudorehearsal. *Connection Science*, 7(2): 123–146, 1995.

Andrei A Rusu, Neil C Rabinowitz, Guillaume Desjardins, Hubert Soyer, James Kirkpatrick, Koray Kavukcuoglu, Razvan Pascanu, and Raia Hadsell. Progressive neural networks. *arXiv preprint arXiv:1606.04671*, 2016.

Pravendra Singh, Vinay Kumar Verma, Pratik Mazumder, Lawrence Carin, and Piyush Rai. Calibrating cnns for lifelong learning. In H. Larochelle, M. Ranzato, R. Hadsell, M.F. Balcan, and H. Lin (eds.), *Advances in Neural Information Processing Systems*, volume 33, pp. 15579–15590. Curran Associates, Inc., 2020. URL `https://proceedings.neurips.cc/paper/2020/file/b3b43aeeacb258365cc69cdaf42a68af-Paper.pdf`.

Cory Stephenson, Abhinav Ganesh, Yue Hui, Hanlin Tang, SueYeon Chung, et al. On the geometry of generalization and memorization in deep neural networks. In *International Conference on Learning Representations*, 2020.

Rufin VanRullen and Ryota Kanai. Deep learning and the global workspace theory. *Trends in Neurosciences*, 44(9):692–704, 2021.

Tom Veniat, Ludovic Denoyer, and MarcAurelio Ranzato. Efficient continual learning with modular networks and task-driven priors. In *International Conference on Learning Representations*, 2020.

Jeffrey S Vitter. Random sampling with a reservoir. *ACM Transactions on Mathematical Software (TOMS)*, 11(1):37–57, 1985.

Zhen Wang, Liu Liu, Yiqun Duan, and Dacheng Tao. Continual learning through retrieval and imagination. In *AAAI Conference on Artificial Intelligence*, volume 8, 2022.

Jaehong Yoon, Eunho Yang, Jeongtae Lee, and Sung Ju Hwang. Lifelong learning with dynamically expandable networks. In *International Conference on Learning Representations*, 2018.

Song Zhang, Gehui Shen, Jinsong Huang, and Zhi-Hong Deng. Self-supervised learning aided class-incremental lifelong learning. *arXiv preprint arXiv:2006.05882*, 2020.

A Analysis of Task-specific Attention Modules

A.1 Selection of appropriate TAM during inference

Continual learning in the brain is mediated by a rich set of neurophysiological processes that harbor different types of knowledge, and conscious processing integrates them coherently. The Global Workspace Theory (GWT) (Baars, 1994) of the conscious information access in the brain states that only the behaviorally relevant information from the perceptual contents in the common representation space are admitted to the global workspace when warranted by a task. However, unless there is sufficient activation in the prefrontal region, information is not always consciously processed in the brain (Juliani et al., 2022). To this end, Global Neuronal Workspace (GNW) hypothesis (Dehaene et al., 1998) posits that brain entails a second computational space composed of widely distributed excitatory neurons that selectively mobilize or suppress, through descending connections, the contribution of specific processor neuron. GNW acts as a router associated with the different brain regions through which the information is selected and made available when triggered by an external stimulus Mashour et al. (2020).

GNW is associated with an *ignition* event (Dehaene et al., 2003) characterized by the activation of subset of workspace neurons and inhibition of the rest of the neurons. Analogously, the TAMs in our network $\tau_\theta = \{\tau_\theta^k \mid k \leq t\}$ act as a communication bottleneck and are associated with an ignition event defined in Equation 5. Although quite simple in its formulation, Equation 5 activates a subset of neurons (an appropriate TAM) and inhibits the rest of neurons (rest of the TAMs) from processing the incoming information. When warranted by a task-specific input, the gating mechanism in Equation 5 allows only the relevant information to pass through the global workspace. The appropriate activation and inhibition of TAMs is quintessential to reducing interference between tasks. As is clear from the experimental evaluation in Table 1, any deviation from the *Oracle* results in higher forgetting. More complex alternatives such as learning a policy using reinforcement learning, a gating mechanism using Gumbel-softmax, and prototype matching can also be explored in place of proposed ignition event to further improve the selection accuracy.

A.2 Choice of TAMs

The prefrontal cortex of the primate brain is presumed to have task-dependent neural representations that act as a gating in different brain functions (Mante et al., 2013). When warranted by a task-specific input, the gating mechanism allows only the relevant information to pass through the global workspace. As noted in Section 3.3, emulating such task-specific attention modules in computational systems comes with several design constraints, including scalability, effectiveness, etc. Table 3 shows some of the TAMs considered in this work. The undercomplete autoencoder (the encoder learns a lower dimensional embedding than input layer) with ReLu nonlinearity as opposed to multilayer perceptron (MLP) or linear layer achieves the best performance. A linear auto-encoder with a Euclidean loss function learns the same subspace as PCA. However, AE with nonlinear functions yields better dimensionality reduction compared to PCA (Hinton & Salakhutdinov, 2006). Therefore, we chose autoencoder with ReLu nonlinearity in the latent stage and sigmoid activation in the output stage as TAM in our proposed approach.

Table 3: Ablations of the different key components of our proposed method. The accuracy is reported on Seq-CIFAR100 for the 500 buffer size learned with 5 tasks.

TAMs	Output non-linearity	Top-1 (%) Seq-CIFAR100 Class-IL
Linear layer	-	41.96 $\pm$2.32
No learnable layer	Sigmoid	42.04 $\pm$0.49
Multi-layer Perceptron	Sigmoid	46.08 $\pm$4.99
Autoencoder	ReLu	44.31 $\pm$0.18
	Tanh	40.78 $\pm$1.56
	Sigmoid	**49.01** $\pm$1.11

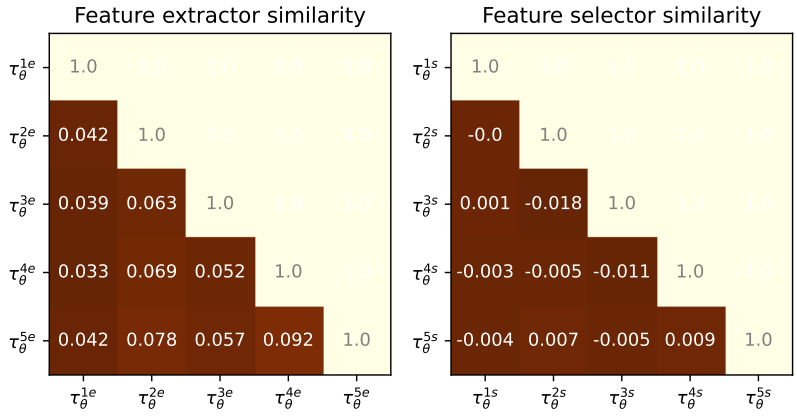

Figure 6: Cosine similarity between different weight feature extractors and selectors of different TAMs under Seq-CIFAR100 (buffer size 500). Although each TAM receives the same input from the common representation space, each TAM learns a different embedding resulting in different attention for each task. Therefore, the cosine similarity between any two TAM is negligibly small.

A.3 TAMs SIMILARITY

We attempt to improve the understanding of TAMs in our proposed method. Each of these TAMs consists of two parts $\tau_\theta^i = \{\tau_\theta^{ie}, \tau_\theta^{is}\}$, where τ_θ^{ie} acts as a feature extractor and τ_θ^{is} as a feature selector. The feature extractor learns a low-dimensional subspace using a linear layer followed by ReLU activation. On the other hand, the feature selector learns task-specific attention using another linear layer followed by sigmoid activation. When using task-specific attention in Class-IL / Task-IL, one would envisage TAMs to capture drastically different information for each task, as each task in Class-IL / Task-IL is vastly different. As the knowledge of the learned tasks is encoded in the weights (Krishnan et al., 2019), we envisage to compute the similarity between weight matrices to gauge whether TAMs are indeed capturing different information. As cosine similarity is widely used in high-dimensional spaces (Luo et al., 2018), we plot the cosine similarity between respective feature extractor and selector weight matrices of each TAMs in Figure 6. As can be seen, all TAMs are vastly different from each other inline with the tasks they were exposed to earlier. We attribute this functional diversity to the pairwise discrepancy loss described in Section 3.3 and Equation 4). As evident in Figure 7, the average activation of the feature extractors begins to diverge from Task-2 as pairwise discrepancy loss kicks in. From Task-2, the average activations are coherent, distributed, and diverse from each other. Due to the limited size of the embedding dimension, there is sparsity in activations in a desirable byproduct.

A.4 PARAMETER GROWTH COMPARISON

We compare the parameter growth in TAMiL with respect to fixed-capacity models and PNNs. Table 4 presents a comparison of parameter growth in 5, 10, and 20 tasks. As the EMA model is not central to the working of our method, we present two versions of TAMiL with and without the EMA model. Compared to a fixed capacity model, TAMiL (without EMA) grows only marginally at 11% even for 20 tasks. Having an EMA model doubles the parameter growth, as both EMA and working model will have same number of TAMs. On the other hand, the number of parameters in PNNs grows exponentially with the number of tasks, thus rendering them inapplicable in real-world scenarios. As shown earlier in Section 5, TAMiL neither suffers from capacity saturation nor from scalability issues, thus producing strong performance even in longer task sequences.

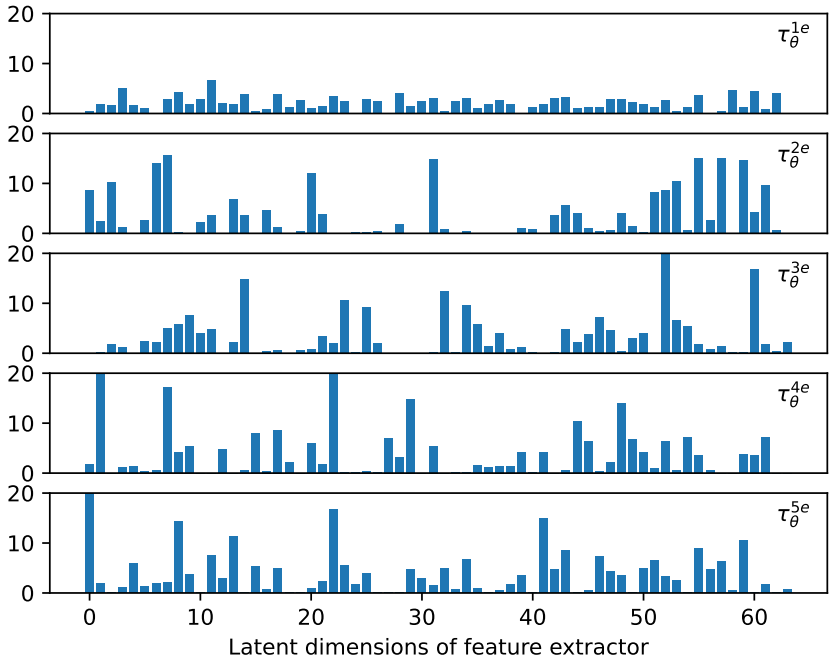

Figure 7: Average activation of feature extractors within each TAM on Seq-CIFAR100. As can be seen, each TAM maps the common representation space to a different latent space thereby reducing the interference. We attribute this behaviour to pairwise discrepancy enforced through Equation 4.

Table 4: Growth in number of parameters for different number of task sequences.

Methods	Number of parameters (Millions)		
	5 tasks	10 tasks	20 tasks
Fixed capacity model	11.23	11.23	11.23
TAMiL (without EMA)	11.55	11.88	12.54
TAMiL (with EMA)	23.10	23.76	25.08
PNNs	297.21	874.01	2645.05

B LIMITATIONS

Inspired by the GWT, we propose TAMiL, a continual learning method that entails task-attention modules to capture task-specific information from the common representation space. Although TAMiL performs extremely well on different CL scenarios, it is not without limitations: TAMiL assumes that common representation space captures the information generalizable across tasks. Violation of this assumption limits the ability of TAMs to capture task-specific information. Secondly, TAMiL requires task boundary information to switch to a new TAM to avoid interference between tasks. We plan to leverage task similarity to merge multiple TAMs into one to avoid this constraint in the future. Finally, As is clear from the experimental evaluation in Table 1, any deviation from the *Oracle* results in higher forgetting. TAMiL can benefit from more accurate matching criterion to match the performance of Oracle. More complex alternatives such as learning a policy using reinforcement learning, a gating mechanism using Gumbel-softmax, and prototype matching can also be explored in place of proposed matching criterion to further improve the selection accuracy.

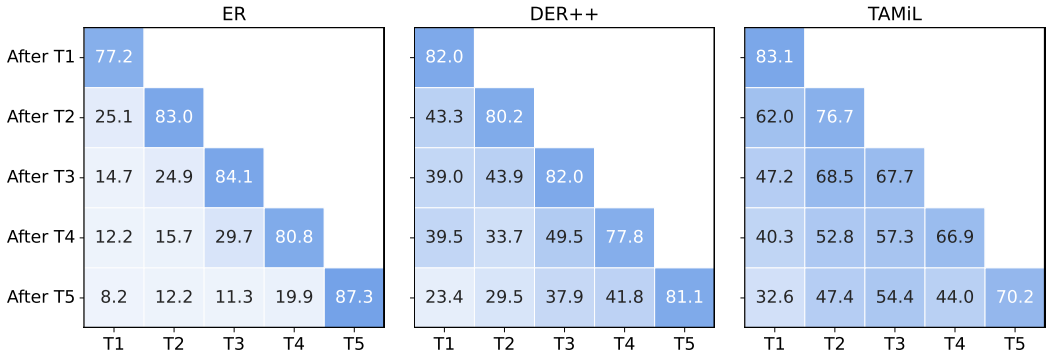

Figure 8: Task-wise performance of CL models trained on Seq-CIFAR100 with buffer size 500 on 5 tasks. The performance of the baseline models is mostly emanating from the performance on the last task while TAMiL achieves considerably more distributed performance on all tasks.

C Prominence of GWT in CL

CL in the brain is mediated by conscious processing of multiple knowledge bases. GWT provides a formal account of cognitive information access and posits that one such knowledge base is a common representation space of fixed capacity from which the information is selected, maintained, and shared with the rest of the brain (Juliani et al., 2022). During information access, the attention mechanism creates a communication bottleneck between the representation space and the global workspace and admits only behaviorally relevant information into the global workspace. Such conscious processing could help the brain achieve systematic generalization (Bengio, 2017) and deal with problems that could only be solved by multiple specialized modules (VanRullen & Kanai, 2021).

In functional terms, GWT as a model of cognitive access has several benefits in CL: (i) the common representation space is largely a shared function, resulting in maximum re-usability across tasks, (ii) the attention mechanism can be interpreted as a task-specific policy for admitting task-relevant information, thereby reducing interference between tasks, and (iii) multiple specialized attention modules enable solving more complex tasks which cannot be solved by a single specialized function. Therefore, we emphasize that emulating GWT in computational models can greatly reduce catastrophic forgetting in CL while leveraging maximum reusability across tasks.

D Task performance

D.1 Task-wise performance

In Table 1, we report the final accuracy after learning all tasks in the Class-IL and Task-IL scenarios. In Figure 8, we disentangle the task-wise performance of different CL models trained on Seq-CIFAR100 with buffer size 500 on 5 tasks. Our proposed method TAMiL retains the performance on previous tasks while the baseline models adapt mostly towards the recent tasks. Therefore, the final average accuracy alone can sometimes be quite misleading.

D.2 Forgetting

While one can argue that learning to classify unseen classes is desirable, Class-IL and Task-IL show distinct classes in distinct tasks, which makes transfer impossible (Buzzega et al., 2020). On the contrary, forgetting is an important measure to gauge the overall performance of the CL model. We compute forgetting as the difference between the current accuracy and its best value for each task. Table 5 presents the forgetting results complementary to the results reported in Table 1. As noted earlier, TAMiL drastically reduces the forgetting, thereby enabling efficient CL with systematic generalization.

Table 5: Forgetting in CL models across various CL scenarios. The results are the average of 3 runs.

Buffer size	Methods	Seq-CIFAR10		Seq-TinyImageNet	
		Class-IL	Task-IL	Class-IL	Task-IL
200	ER	61.24±2.62	7.08±0.64	76.37±0.53	43.14±0.97
	DER++	32.59±2.32	5.16±0.21	72.74±0.56	41.63±1.13
	TAMiL	**22.03** ± 1.89	**3.45** ±0.39	**55.69**±1.45	**24.54**±0.94
500	ER	45.35±0.07	3.54±0.35	75.27±0.17	31.36±0.27
	DER++	22.38±4.41	4.66±1.15	64.58±2.01	27.85±0.51
	TAMiL	**15.95**±0.86	**3.14**±0.42	**43.43**±2.24	**15.68**±0.18

Table 6: Comparison of CL models in three different settings: Single head, Multi-head and Single head with TAMs.

Buffer size	Methods	Single head	Multi-head	With TAMs (Single head)
500	ER	68.23±0.17	68.15±0.31	**69.15** ±0.72
	DER++	70.61±0.08	75.58±0.30	**77.47** ±0.28
	CLS-ER	-	79.58 ±0.38	**79.62**±0.11

D.3 Performance on Seq-core50

Table 7 provides a comparison of different Cl models on Seq-core50. Following Maltoni & Lomonaco (2019), Seq-Core50 is organized into nine tasks, the first of which includes ten classes, while the rest have five classes each. As can be seen, TAMiL improves the performance in most settings. In the oracle version, using a task-specific TAM greatly improves performance, as much as 30% in the Class-IL scenario.

D.4 Comparison with multi-head setup

We seek to provide an understanding of how task-specific parameters improve learning in sequential tasks. Table 6 describes an ablation of three baseline methods namely ER, DER++ and CLS-ER in presence of multiple heads in Task-IL setting. Each method was evaluated under single-head setting, multi-head setting and single-head with TAMs setting. As per CLS-ER original formulation, we evaluate EMA model instead of the working model. As can be seen, TAMs bring discernible performance improvement over multi-head setting. We attribute this to the ability of TAMs to capture task-specific information better without overfitting on the limited labels from the buffer. In the future, a comprehensive method which includes both multiple-heads and TAMs can be developed to further improve the performance of CL models.

Table 7: Comparison of CL models on Seq-core50. We provide the average Top-1 (%) accuracy of all tasks after CL training.

Buffer size	Methods	Seq-Core50	
		Class-IL	Task-IL
200	ER	21.49±0.56	65.63±0.92
	DER++	28.47±0.61	68.50±1.03
	TAMiL	**32.67**±0.36	**70.76** ±1.05
	TAMiL (Oracle)	**64.04**±1.34	70.53±0.47
500	ER	29.39±0.77	69.90±0.95
	DER++	**40.31**±1.49	75.94±0.24
	TAMiL	39.15±1.48	**77.36** ±0.60
	TAMiL (Oracle)	**70.90** ±0.43	76.53±0.20

Algorithm 2 Reservoir sampling (Vitter, 1985)

input: Data streams $\mathcal{D}_t$, $\mathcal{D}_m$, $\{x, y\} \in \mathcal{D}_t$
Maximum buffer size $\mathcal{M}$, current buffer size $\mathcal{N}$
if $\mathcal{M} > \mathcal{N}$ **then**
    $\mathcal{D}_m[\mathcal{N}] \leftarrow \{x, y\}$
else
    $v = randomInteger(min = 0, max = \mathcal{N})$
    if $v < \mathcal{N}$ **then**
        $\mathcal{D}_m[v] \leftarrow \{x, y\}$
return $\mathcal{D}_m$

E IMPLEMENTATION DETAILS

E.1 RESERVOIR SAMPLING

Algorithm 2 describes the steps for building a memory buffer using the reservoir sampling strategy (Vitter, 1985). Reservoir sampling assigns equal probability to each sample of a data stream of unknown length to be represented in the memory buffer. When the buffer is full, the replacements are made randomly.

E.2 DATASETS AND MODEL

We obtain Seq-CIFAR10, Seq-CIFAR100 and Seq-TinyImageNet by splitting CIFAR10 (Krizhevsky et al., 2009), CIFAR100 (Krizhevsky et al., 2009) and TinyImageNet (Le & Yang, 2015) into 5, 5 and 10 partitions of 2, 20 and 20 classes per task, respectively. We also experiment with longer task sequences in Seq-CIFAR100 by increasing number of tasks to 5, 10 and 20 while correspondingly decreasing number classes to 20, 10, and 5, respectively. Following Arani et al. (2022); Buzzega et al. (2020); Cha et al. (2021); Caccia et al. (2021a), we employ ResNet-18 (He et al., 2016) as the backbone to learn a common representation space for all our experiments. We use a single, expanding linear classifier representing all classes belonging to all tasks. The training regime for both Class-IL and Task-IL are as follows: The CL model is trained on all tasks sequentially with/without experience-rehearsal with reservoir sampling depending on its formulation. During training, entire network is updated including the linear classifier. The training scheme is same for both Class-IL and Task-IL. For comparison between different state-of-the-art methods, we report the average of accuracies on all tasks seen so far in Class-IL. As is the standard practice in Task-IL, we leverage the task-identity and mask the neurons that do not belong to the prompted task in the linear classifier.

Our CL model consists of as many TAMs as the number of tasks. Each TAM is an auto-encoder with a linear layer with relu activation as an encoder and a linear layer with sigmoid activation as a decoder. Both input and output are 512 dimensional while the latent space is of 64 dimensions. As TAMiL involves an EMA model for consistency regularization, we use CLS-ER's two-model version with a single EMA copy for a fair comparison. As TAMs can be plugged on top of any rehearsal-based approach, we look to improve multiple-EMA CLS-ER with TAMs in the future.

E.3 BACKBONES USED FOR COMPARISON WITH DYNAMIC SPARSE NETWORKS

Diverging from the mainstream practice of utilizing a dense CL model, dynamic sparse approaches start with a sparse network and maintain the same connection density throughout the learning trajectory. As sparsifying a CL model involves disentangling interfering units to avoid forgetting, and creating novel pathways to encode new knowledge, implementing batch normalization and residual connections is not trivial for both NISPA and CLNP. Therefore, these methods do not use ResNet-18 architecture. Instead, they opted for a simple CNN architecture without skip connections and batch

normalization. On the other hand, TAMiL is not prone to the complexities in the underlying model and is therefore simple to plug-and-play for any approach with any kind of backbone.

E.4 MAINTAINING AN EMA MODEL FOR CONSISTENCY REGULARIZATION

Knowledge of the previous tasks can be better preserved using consistency regularization in CL (Bhat et al., 2022). To enforce consistency, either the previous predictions can be stored alongside the image in the buffer or an EMA teacher model can be employed to distill the knowledge about the previous tasks. In DER++, previous predictions are stored in the buffer. In Figure 3(left) we plug-and-play TAMs on top of DER++ and show discernible improvement, indicating that the effectiveness of TAMs is independent of the use of EMA model.

The EMA of a model can be considered as forming a self-ensemble of the intermediate model states that leads to better internal representations (Arani et al., 2022). Therefore, using an EMA model instead of storing the logits yields better results in CL. Therefore, we use an EMA model in all our experiments in Table 1. While training a CL model in TAMiL, we stochastically update the EMA model as follows:

$$\theta_{EMA} = \begin{cases} \theta_{EMA}, & \text{if } \gamma \geq \mathcal{U}(0,1) \\ \eta\, \theta_{EMA} + (1-\eta)\, \theta, & \text{otherwise} \end{cases} \tag{7}$$

where η is a decay parameter, γ is a update rate and, θ and θ_{EMA} represent weights of CL model and EMA model respectively. During each iteration, buffered input is passed through each of these models and CL model's predictions are enforced to be consistent with the EMA model's predictions.